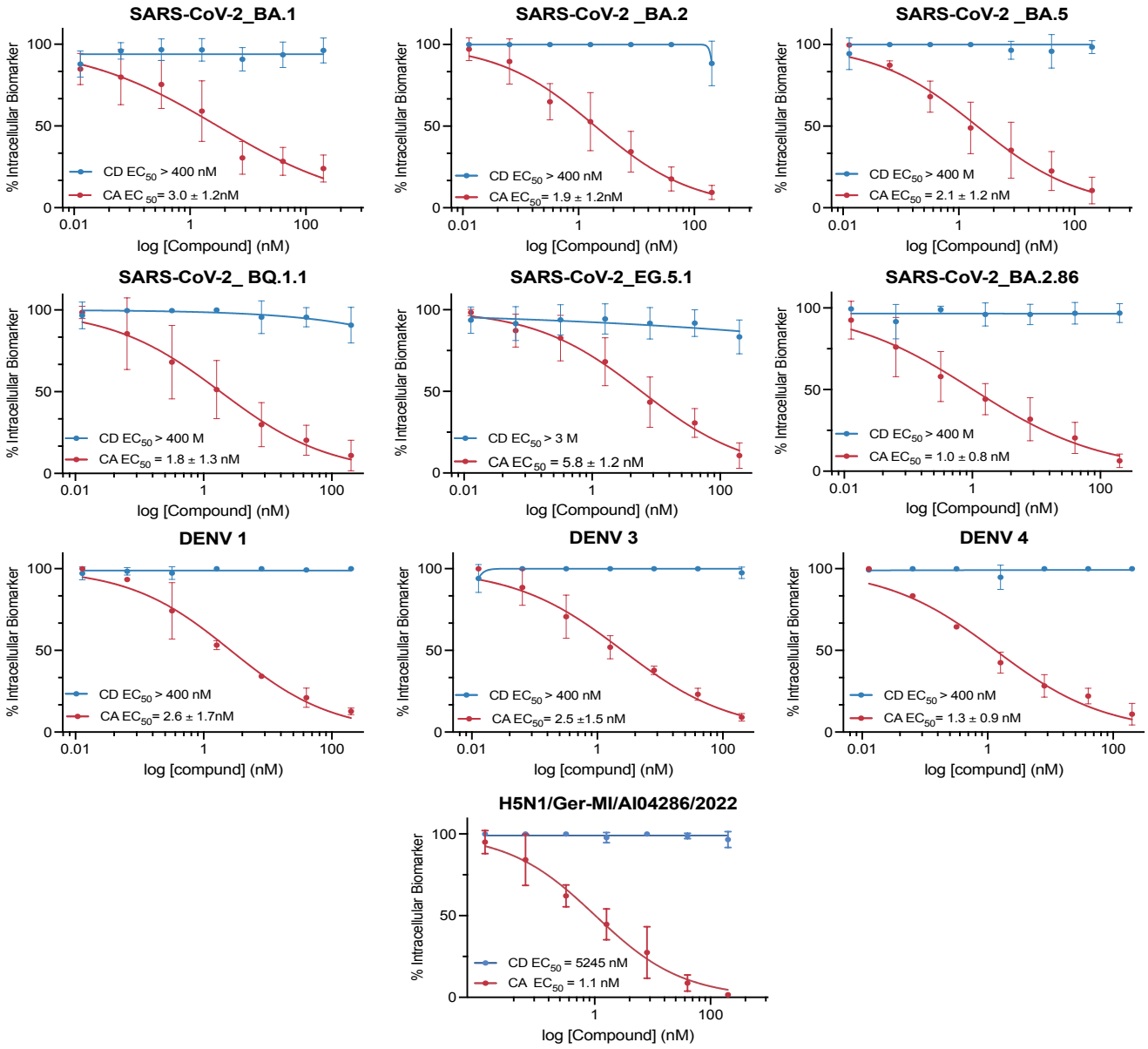

Figure S1. CA broad-spectrum antiviral. Dose-response curves of cells pretreated with the indicated concentrations of CA or CD before infection with indicated virus using viral proteins as infection markers. EC_{50} values were determined using nonlinear regression analysis. The GraphPad Prism 10™ (GraphPad Software, Inc.) nonlinear regression fit modelling variable slope was used to generate a dose-response curve [Y = Bottom + (Top-Bottom)/(1+10^((LogIC50-X)*HillSlope)] constrained to top = 100, bottom = 0. (n = 3).

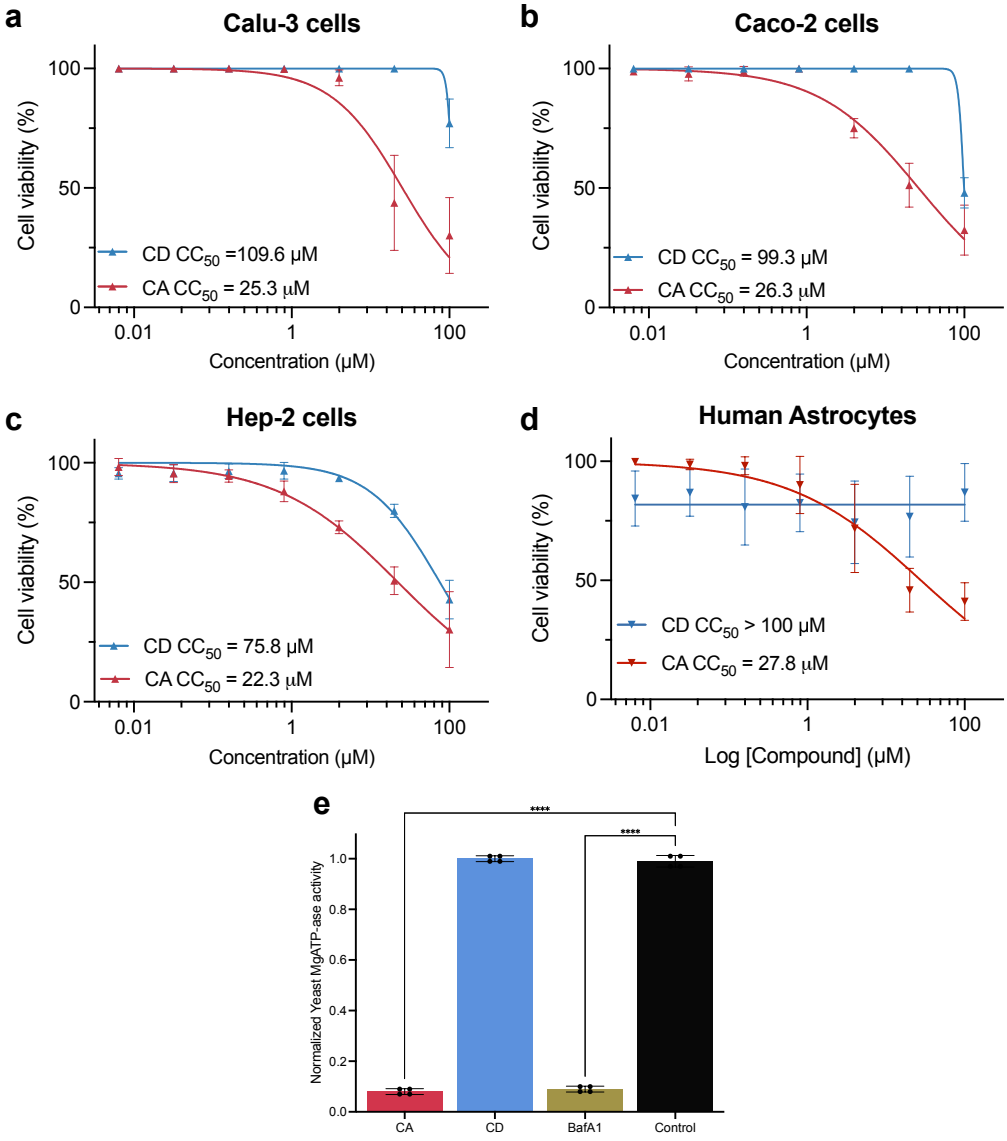

Figure S2. **Cytotxic assays and yeast V-ATPase activity.** Cell viability were generated for the indicated serial diluted CA (red) and CD (blue) in (**a**) Calu-3 cells, (**b**) Caco-2 cells, (**c**) Hep-2 cells and (**d**) human astrocytes. CC_{50} values were determined using nonlinear regression analysis. The GraphPad Prism 10™ (GraphPad Software, Inc.) nonlinear regression fit modeling variable slope was [Y = Bottom + (Top-Bottom)/(1+10^((LogIC50-X)*HillSlope)] constrained to top = 100, bottom = 0. The graph shows the average values of three independent experiments. **e**) Inhibition by CA, bafA1 and not CD, of the reconstituted yeast V-ATPase.

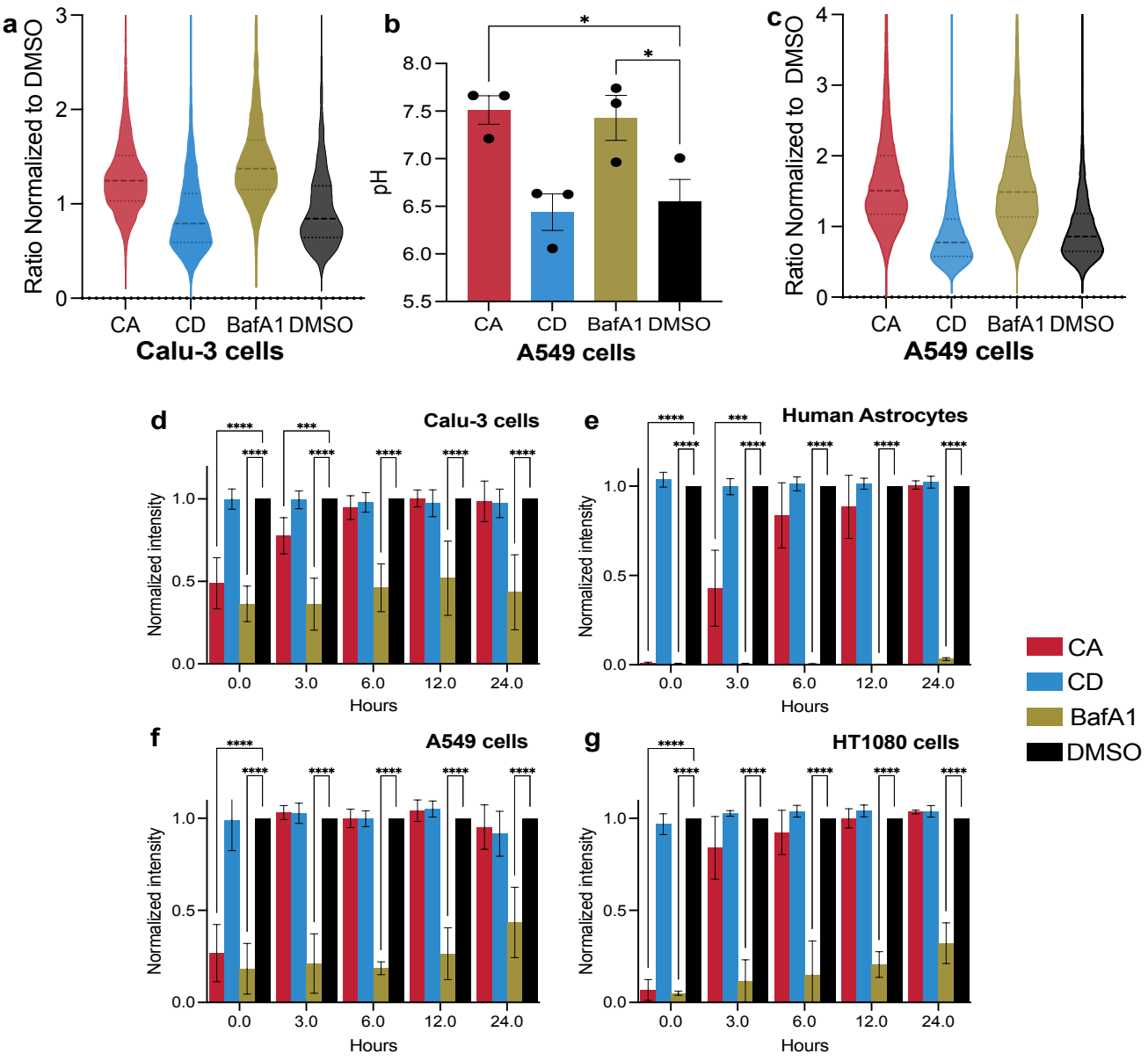

Figure S3. Effect of CA in intracellular pH. The pH of intracellular vesicles was measured using confocal imaging of Calu-3 cells (**a**) and A549 cells (**b-c**) treated with a pH-sensitive indicator (FITC-labelled 70kDA dextran); fluorescence intensity at excitation 488nm is divided by excitation at 458nm to extract pH-related ratios. The pH of intracellular vesicles was measured using confocal imaging of cells treated with a pH-sensitive indicator (FITC-labelled 70kDA dextran); Fluorescence intensity at excitation 488nm is divided by excitation at 458nm to extract pH-related ratios. Overall, this assay demonstrated that pH is increased relative to controls following treatment with CA or BafA. Endolysosomal pH was assessed at 0, 3, 6, 12 and 24 h after 3h preincubation of the compounds in Calu-3 cells (**d**), human astrocytes (**e**), A549 cells (**f**) and HT1080 cells (**g**). The total intensity of the acridine orange spots per cell was obtained using the CellInsight CX7 HCS platform. A one-way ANOVA was used to determine significant differences for n = 3 experiments. Only P values less than 0.005 are shown (**** $p < 0.0001$; ***$p \leq 0.001$, **$p \leq 0.01$, *$p \leq 0.05$).

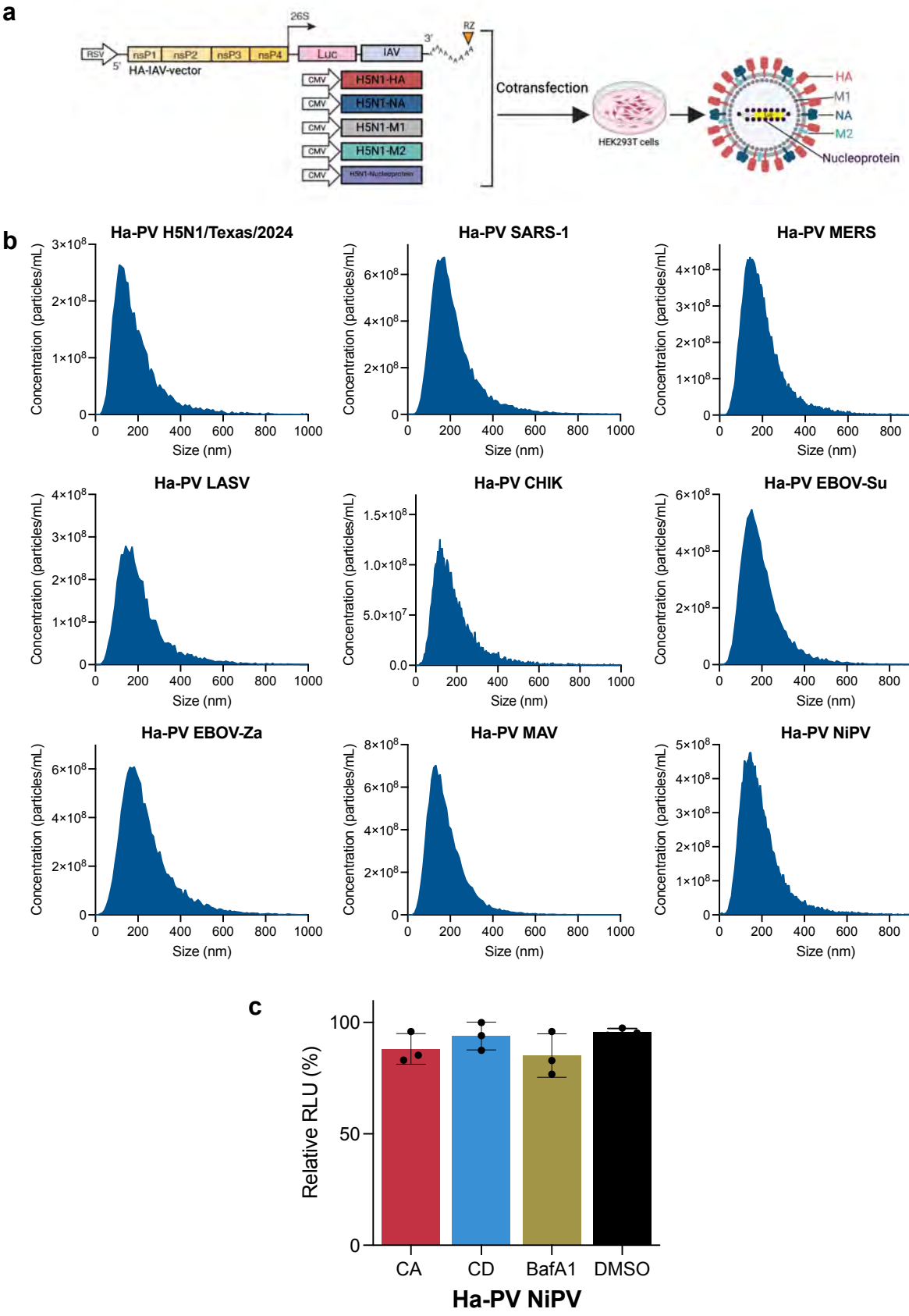

Figure S4. Entry inhibition of pseudoviruses. **a**) Illustration of the design of Ha-H5N1 vector. The vector contains an RSV promoter that transcribes the full-length viral RNA genome to be packaged into Ha-H5N1 particles. Shown is the 5' untranslated region followed by open-reading frames coding for nonstructural proteins (nsps) 1–4 from Semliki Forest virus (SFV), viral subgenomic promoters for Luc or RFP reporter expression, the 3' untranslated region, and a poly(A) tail that is self-cleaved by the hepatitis delta virus ribozyme (RZ). The A/Texas/37/2024 H5N1 -packaging signal is inserted in front of the 3' untranslated region. To assemble viral particles, HEK293T cells were co-transfected with Ha-H5N1 and the vectors expressing the 5 structural proteins of A/Texas/37/2024 H5N1 (HA, NA, M1, M2 and N). Modifiy from Hetrick et.al 2022. **b**) Nanoparticle Tracking Analysis (NTA) performed in Ha-PV. **c**) Cells were pretreated for 1h with 200nM of inhibitors before 18h infection with Ha-PV-(Luc). Viral entry inhibition was quantified by luciferase assay. Data are normalized to quantify luciferase with only pseudovirus. A one-way ANOVA was used to determine significant differences. Only p values less than 0.05 are shown (****p<0.0001).

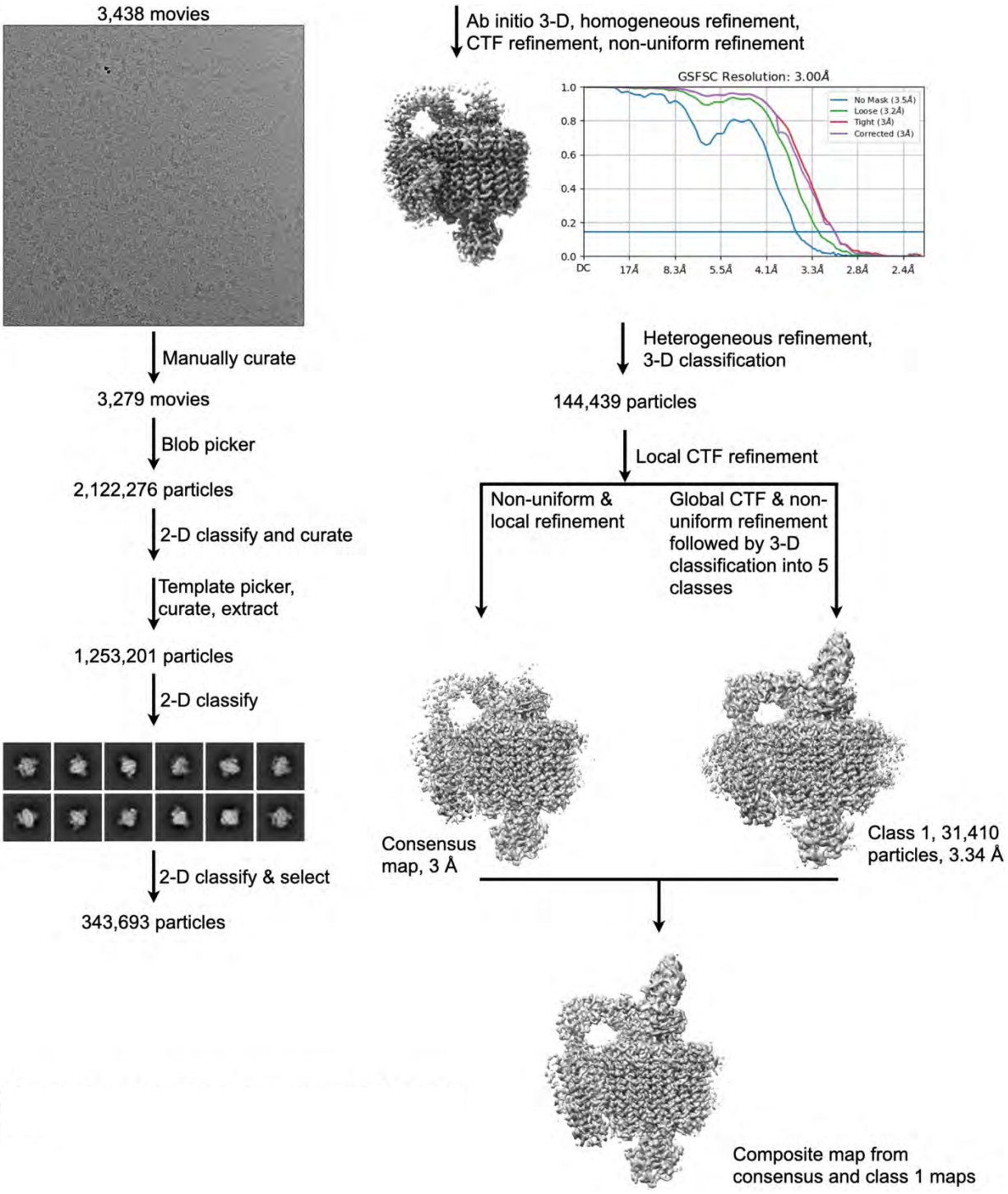

Figure S5. CryoEM structure determination of CA bound HsV_oND

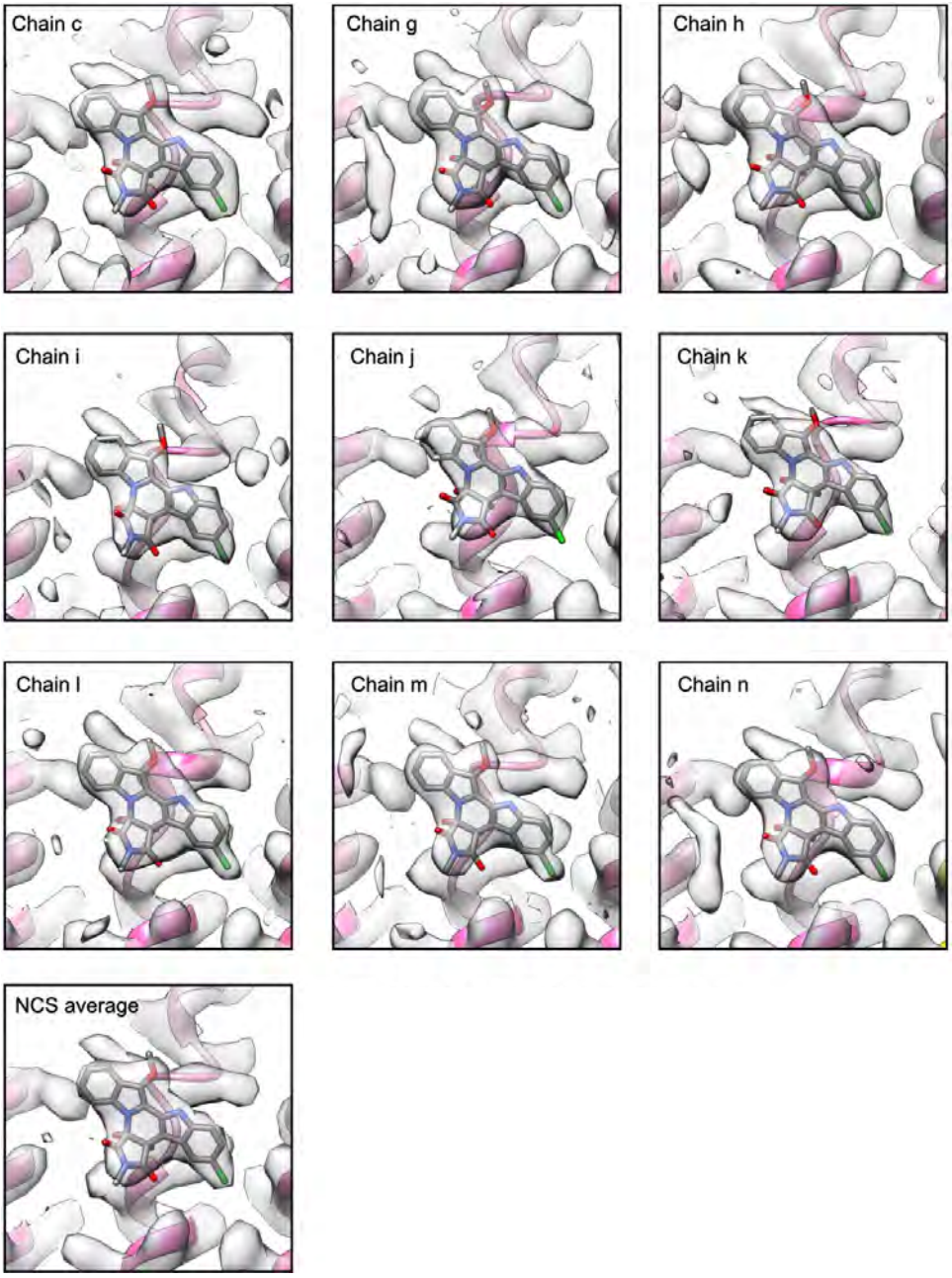

Figure S6. EM density for CA molecules 1-9. EM density for CA molecules bound to c subunit chains 1-9. NCS map averaging was used for the bottom left panels.

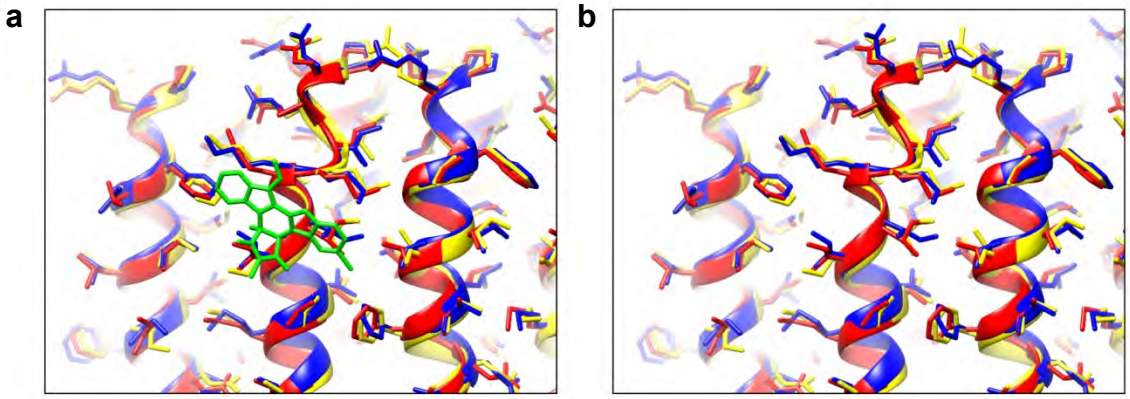

Figure S7. Comparison of CA model bound *c* subunits of Vo of human V-ATPase in detergent (a; pdbid:6wm2) and lipid nanodisk (b;pdbid: 7unf). CA binding is mostly to α helix 2 of the c subunit, with the chloride moiety contacting helix 4 of a neighboring c subunit. c subunit are averlaid in chimers, with the model of CA bound in yellow, c from models 6wm2 and 7unf in red and blue, respectively.

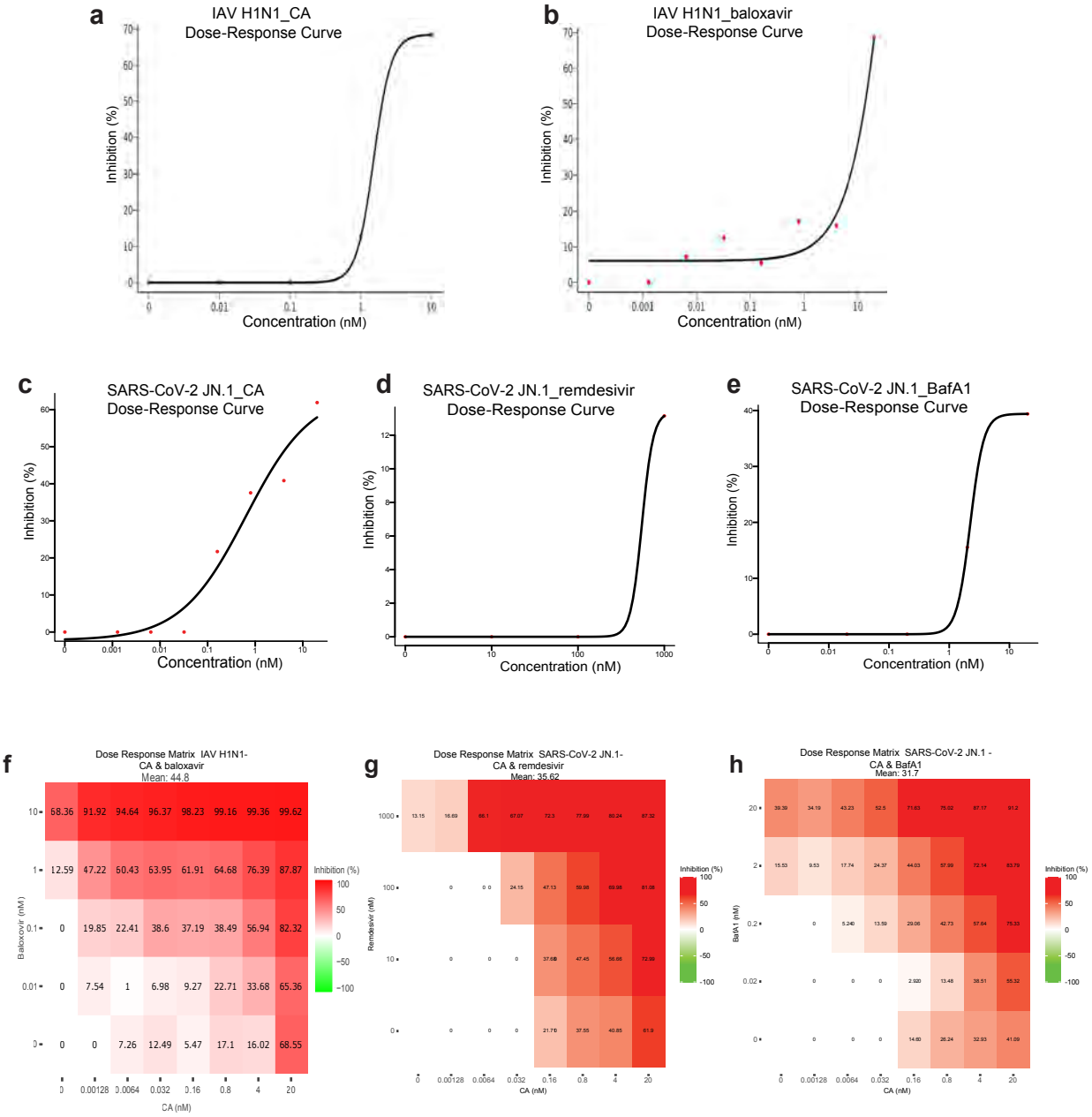

i Synergy Score Summary Table

	ZIP	Loewe	HAS	Bliss
CA/baloxavir	22.76	23.11	24.98	21.88
CA/remdesivir	19.34	10.24	20.92	19.43
CA/bafA1	11.9	13.83	15.32	11.34

Figure S8. Synergistic inhibition of SARS-CoV-2 Omicron JN.1 infection in human lung Calu-3 cells by combined use of CA and nirmatrelvir, remdesivir or BafA1. **a-e)** Dose-response curves of inhibition of single treatment of CA, baloxovir, remdesivir and BafA1 in IAV H1N1 & SARS-CoV-2 JN.1 infected Calu-3 cells.

f-h) Dose-response matrix (percentage inhibition) of IAV H1N1 and SARS-CoV-2 JN.1 infection with combined treatment of CA with baloxovir, remdesivir or BafA1.**i)** Synergy score summary table for the four synergy methods used.